

Discrete Signal Processing on Meet/Join Lattices

Markus Püschel, *Fellow, IEEE*, Bastian Seifert, *Member, IEEE*, and Chris Wendler, *Student Member, IEEE*

Abstract—A lattice is a partially ordered set supporting a meet (or join) operation that returns the largest lower bound (smallest upper bound) of two elements. Just like graphs, lattices are a fundamental structure that occurs across domains including social data analysis, natural language processing, computational chemistry and biology, and database theory. In this paper we introduce discrete-lattice signal processing (DLSP), an SP framework for data, or signals, indexed by such lattices. We use the meet (or join) to define a shift operation and derive associated notions of filtering, Fourier basis and transform, and frequency response. We show that the spectrum of a lattice signal inherits the lattice structure of the signal domain and derive a sampling theorem. Finally, we show two prototypical applications: spectral analysis of formal concept lattices in social science and sampling and Wiener filtering of multiset lattices in combinatorial auctions. Formal concept lattices are a compressed representation of relations between objects and attributes. Since relations are equivalent to bipartite graphs and hypergraphs, DLSP offers a form of Fourier analysis for these structures.

I. INTRODUCTION

WE have entered the age of big data and signal processing (SP) as a classical data science is a key player for data analysis. One main challenge is to broaden the foundation of SP to become applicable across the large variety of data available.

Classical SP and many of its applications are built on the fundamental concepts of time- or translation-invariant systems, convolution, Fourier analysis, sampling, and others. But many data sets are not indexed by time, or its separable extensions to 2D or 3D. Thus an avenue towards broadening SP is in porting these concepts to index domains with inherently different structures to enable the power of the numerous SP techniques that build on these concepts.

Graph signal processing and beyond. A prominent example of this approach is graph signal processing (GSP) [1], [2], which considers data indexed by the nodes of a graph. It replaces the time shift or translation by the adjacency or Laplacian operator, whose eigendecomposition yields the Fourier transform. Polynomials in

the operator yield the associated notion of convolution. Building on these concepts, numerous follow-up works have reinterpreted and ported many classical SP tools to GSP [3].

However, not all index domains are graphs or a graph may be the wrong abstraction. Thus, there have been various recent works that aim to further broaden SP beyond graphs. Examples include SP on hypergraphs [4], graphons [5], simplicial complexes [6], so-called quivers [7], and powersets [8]. Some of the above works have been inspired by the algebraic signal processing theory (ASP) [9], [10], which provides the axioms and a general approach to obtaining new SP frameworks. In particular, ASP identifies the shift operator (or operators) as key axiomatic concept from which convolution, Fourier analysis, and other concepts can be derived. Early examples derived SP frameworks on various path graphs [11], [12] or regular grids [13].

Meet/join lattices. In this paper we consider signals, or data, indexed by meet/join lattices, a fundamental structure across disciplines. A lattice is a partially ordered set that supports a meet (join) operation that returns for each pair of elements their largest lower bound (smallest upper bound). We provide a few examples.

Formal concept lattices [14] are used in social data analysis. Such a lattice distills relations between objects (e.g., users) and attributes (e.g., likes a certain website) into so-called concepts. Relations can be viewed as tables with binary entries and are equivalent to bipartite graphs or hypergraphs. Formal concept lattices also play a role in the emerging field of granular computing in information processing [15].

Ranked data [16] can be viewed as indexed by the set of permutations, which form a lattice, partially ordered by the number of neighbor exchanges they consist of.

The set of partitions of a finite set form a lattice, which is fundamental in database theory [17].

In combinatorial chemistry some reaction networks form a lattice [18], whose elements are chemical structures. Lattice signals can then represent chemical properties, e.g., retention indices.

In evolutionary genetics a gene and its genotypes, i.e., variations by mutations, form a lattice [19], [20].

The authors are with the Department of Computer Science, ETH Zurich, Switzerland (email: pueschel@inf.ethz.ch, bastian.seifert@inf.ethz.ch, chris.wendler@inf.ethz.ch)

Phenotypes, such as resistance to certain drugs, are then naturally represented by lattice signals [21].

In natural language processing lattices occur naturally, e.g., the prefix order on words with a meet operation that returns the longest common prefix [22].

Every tree defines a lattice, with the root as largest element and the join of two nodes as the closest common ancestor. Data on trees is ubiquitous.

Contribution: Discrete-lattice SP (DLSP). In this paper we present a novel linear SP framework, called DLSP, for signals indexed by finite meet/join lattices. First, we derive the theory using the general high-level procedure provided by ASP [9]. Namely, we use the meet (or join) operation to define a notion of shift, from which we derive the associated notions of convolution, Fourier basis, Fourier transform, frequency response, and others. Using the concept of total variation, we show that the spectrum is again partially ordered and forms a lattice isomorphic to the signal domain. We derive a sampling theorem for signal with known sparse Fourier support.

In the second part we show two possible application domains: spectral analysis of formal concepts lattices occurring in social data analysis and sampling and Wiener filtering of multiset lattices occurring in combinatorial auctions. Formal concept lattices are particularly interesting as they distill relations between objects and attributes into a lattice. Since relations are equivalent to bipartite graphs and hypergraphs, DLSP offers a form of Fourier analysis for data indexed by these structures.

This paper extends and completes the preliminary work in [23], [24].

II. BACKGROUND ON LATTICES

In this section we provide the necessary basic background on semilattices and lattices. Lattice theory is a well-studied area in mathematics. Good reference books are [25], [26], which also give an idea of the rich theory available for lattices.

Partially ordered sets. We consider finite sets \mathcal{L} with a *partial order* \leq , also called *posets*. We denote elements of \mathcal{L} with lower case letters a, b, x, \dots . Formally, a poset satisfies three axioms for all $a, b, c \in \mathcal{L}$:

- 1) $a \leq a$,
- 2) $a \leq b$ and $b \leq a$ implies $a = b$, and
- 3) $a \leq b$ and $b \leq c$ implies $a \leq c$.

We will use $a < b$ if $a \leq b$ but $a \neq b$.

We say that b covers a , if $a < b$ and there is no $x \in \mathcal{L}$ with $a < x < b$. Equivalently, a is a largest element (there could be several) below b .

Meet-semilattice. A meet-semilattice is a poset \mathcal{L} that also permits a meet operation $a \wedge b$, which returns the greatest lower bound of a and b , which thus must be unique. Formally, it satisfies for all $a, b, c \in \mathcal{L}$:

- 1) $a \wedge a = a$,
- 2) $a \wedge b = b \wedge a$, and
- 3) $(a \wedge b) \wedge c = a \wedge (b \wedge c)$.

The latter two show that \wedge is commutative and associative.

Using the notion of cover, semilattices can be visualized through a directed acyclic graph $(\mathcal{L}, \mathcal{E})$ called cover graph. The nodes are the elements of \mathcal{L} and $(b, a) \in \mathcal{E}$ if b covers a . The elements of \mathcal{E} are called covering pairs. The graph is typically drawn in a way that if $a \leq b$, then b is higher than a .

Fig. 1a shows a small example of a meet-semilattice. The cover graph shows, e.g., that $c \leq f, b \leq h, c \not\leq g$ and further $e \wedge f = b, h \wedge g = a$, etc. Note that a meet semilattice must have a unique smallest element \min , which is the meet of all elements in \mathcal{L} . In Fig. 1a this is a .

Lattice. Dual to the meet-semilattice, one can define a *join-semilattice* as a poset with an operation \vee that returns the least upper bound and satisfies analogous properties and necessarily has a unique maximal element. If a finite poset supports both a meet and a join operation, it is called a *lattice*. Fig. 1a is not a join semilattice since the join of g and h does not exist.

In the case of finite lattices \mathcal{L} considered here, the difference between semilattices and lattices is marginal. More precisely, the following holds:

Lemma 1. *Every meet-semilattice with a unique maximal element \max , i.e., $\max \geq a$ for all $a \in \mathcal{L}$, is a lattice. Namely, if $a^u = \{x \in \mathcal{L} \mid x \geq a\}$, then the join of a and b can be computed as*

$$a \vee b = \bigwedge a^u \cap b^u.$$

The maximum ensures that $a^u \cap b^u$ is not empty. As a consequence we can always extend a meet-semilattice to a lattice by adding a artificial maximal element if it does not exist.

Examples. If the partial order is a total order, i.e., for all distinct $a, b \in \mathcal{L}$ either $a \leq b$ or $b \leq a$, then \mathcal{L} is a lattice. An example is shown in Fig. 1b with four elements.

Another special case of a lattice is the power set (set of all subsets) of a finite set \mathcal{S} with \cap as meet and \cup as join, which yields a directed hypercube as associated cover graph. Fig. 1c shows the example for $\mathcal{S} = \{\alpha_1, \alpha_2, \alpha_3\}$: here, $a = \emptyset$, b, c, d are the one-element subsets, e, f, g the two-element subsets, and $h = \mathcal{S}$. Signals indexed by power sets are called set functions. We introduced an SP framework for set functions in [8], [27]. The work in this paper generalizes to arbitrary meet- or join-semilattices.

Not every poset with unique minimal element is a meet-semilattice. For example, Fig. 1d is not since the meet of d and e is not unique.

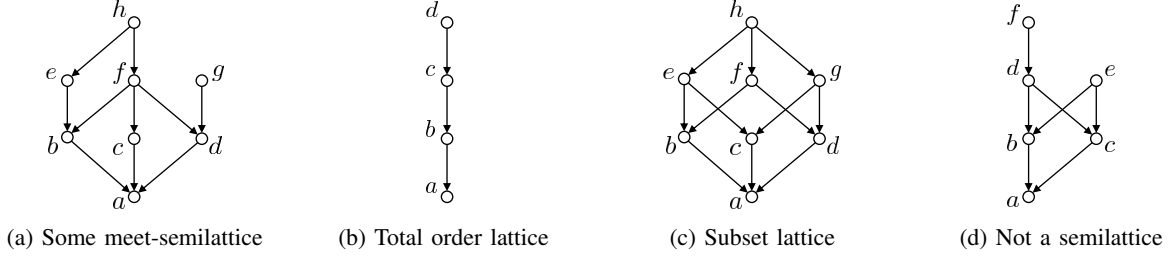


Fig. 1: Examples of semilattices \mathcal{L} . The labels are the names of the nodes, i.e., elements of \mathcal{L} . In this paper, we consider signals on \mathcal{L} that associate values which each node.

We will provide more concrete examples of lattices including multiset, and concept lattices later in our application section.

Some properties. The cover graphs associated with meet-semilattices are acyclic and, as said above, have a unique sink (node with outdegree 0). However, these properties are not sufficient as shown in Fig. 1d.

Every poset can be topologically sorted, i.e., can be totally ordered in a way that is compatible with the partial order. In Fig. 1 this is done with the lexicographic order of the node labels, meaning smaller elements in the poset come earlier in the alphabet. In general, the topological sort is not unique.

III. DISCRETE-LATTICE SP

In this section we introduce discrete-lattice SP¹ (DLSP), a signal processing framework for signals, or data, associated with the elements of a given meet- or join-semilattice. DLSP could also be viewed as a form of graph SP on the special type of directed acyclic graphs that are associated with semilattices (e.g., those in Fig. 1). We discuss the differences to prior digraph SP frameworks later.

Our derivation of DLSP follows the general procedure of ASP [9], [10] for deriving linear SP frameworks. We start with the shift definition, from which we then derive the associated notions of convolution or filtering, Fourier transform, frequency response, and convolution theorems.

In the next section we then provide a detailed example.

Lattice signals. We consider real signals indexed with the elements of a given meet-semilattice \mathcal{L} of size n :

$$\mathbf{s} : \mathcal{L} \rightarrow \mathbb{R}, \quad x \mapsto s_x. \quad (1)$$

We will also write $\mathbf{s} = (s_x)_{x \in \mathcal{L}}$, considered as a column vector, where we assume a specific order in which the elements are topologically sorted from small to large. The set of signals is an n -dimensional vector space.

¹More correct would be discrete-semilattice SP, but we opted for simplicity.

Shifts. Our construction uses the meet operation to define a shift. Formally, for every $a \in \mathcal{L}$ we define the

$$\text{shift by } a: (s_x)_{x \in \mathcal{L}} \rightarrow (s_{x \wedge a})_{x \in \mathcal{L}},$$

which captures the semilattice structure. Obviously, this shift is a linear mapping on the signal space since shifting $\alpha \mathbf{s} + \beta \mathbf{s}'$ ($\alpha, \beta \in \mathbb{R}$) by a yields $\alpha(s_{x \wedge a})_{x \in \mathcal{L}} + \beta(s'_{x \wedge a})_{x \in \mathcal{L}}$. Thus, the shift by a is represented by a matrix T_a and

$$T_a \mathbf{s} = (s_{x \wedge a})_{x \in \mathcal{L}}.$$

The definition implies the following property for $a, b \in \mathcal{L}$

$$T_a(T_b \mathbf{s}) = T_{a \wedge b} \mathbf{s} = T_b(T_a \mathbf{s}). \quad (2)$$

If \mathcal{L} contains a maximal element max , then $T_{max} \mathbf{s} = \mathbf{s}$ is the identity mapping.

Generating shifts. In discrete-time SP a signal can be shifted by any integer value, but each such shift can be expressed as a repeated shift by 1, i.e., the shift by 1 *generates* all others. The question is which shifts in our lattice are needed to generate all others. Equation (2) shows that a shift by $a \wedge b$ can be done by shifting by a and then by b and thus is not needed as generator. Thus, as explained by lattice theory [26], the generators are precisely all meet-irreducible elements, i.e., those $a \in \mathcal{L}$ that cannot be written as $a = b \wedge c$ with $b, c \neq a$. This definition does not include a unique maximal element if \mathcal{L} has one.

In Fig. 1a the basic shifts that generate all others are thus given by h, e, f, g, c . In Fig. 1b these are all elements except d , and in Fig. 1c they are e, f, g .

Filters and convolution. The associated notion of convolution is obtained by linearly extending the shift operation to filters $\sum_{a \in \mathcal{L}} h_a T_a$. Convolution then is defined as

$$\mathbf{h} * \mathbf{s} = \left(\sum_{a \in \mathcal{L}} h_a T_a \right) \mathbf{s} = \left(\sum_{a \in \mathcal{L}} h_a s_{x \wedge a} \right)_{x \in \mathcal{L}}.$$

Shift-invariance. Since the meet operation is commutative, all shifts commute with each other and thus also with all filters, in other words, DLSP is shift-invariant.

Fourier basis and frequency response. To derive the associate Fourier transform we first determine the Fourier basis, i.e., the signals that are simultaneous eigenvectors for all shifts (in particular the generating shifts) and thus for all filters. Note that their existence is possible since the shifts commute, see (2). Lattice theory confirms the existence of a joint eigenbasis through the zeta transform [28]. Translated to our SP setting, there is a Fourier basis vector \mathbf{f}^y for every $y \in \mathcal{L}$, defined as

$$\mathbf{f}^y = (\iota_{y \leq x})_{x \in \mathcal{L}}. \quad (3)$$

Here, $\iota_{y \leq x}$ is the characteristic (or indicator) function of $y \leq x$:

$$\iota_{y \leq x} = \iota_{y \leq x}(x, y) = \begin{cases} 1, & y \leq x, \\ 0, & \text{else.} \end{cases}$$

In words, the signal \mathbf{f}^y consists only of entries 1 and 0, depending on the condition $y \leq x$. In particular, for the unique minimal element $\min \in \mathcal{L}$

$$\mathbf{f}^{\min} = (1, 1, \dots, 1)^T$$

is the constant vector.

To show that \mathbf{f}^y is an eigenfunction for all shifts, we choose some $a \in \mathcal{L}$ and get

$$T_a \mathbf{f}^y = (\iota_{y \leq x \wedge a})_{x \in \mathcal{L}} = \begin{cases} \mathbf{f}^y, & y \leq a, \\ 0, & y \not\leq a. \end{cases} \quad (4)$$

The last equality is explained as follows. If $y \leq a$, then $y \leq x \wedge a \Leftrightarrow y \leq x$ and thus the result is \mathbf{f}^y . This means the frequency response of a shift by such an a is 1. If $y \not\leq a$, then $y \leq x \wedge a$ never holds and the result is the zero vector. This means the frequency response of a shift by such an a is 0.

Hence, by linear extension, the frequency response of a filter $\mathbf{h} = (h_a)_{a \in \mathcal{L}}$ at frequency y is computed as

$$\bar{h}_y = \sum_{a \in \mathcal{L}, a \geq y} h_a. \quad (5)$$

Frequency ordering. An important aspect for a useful SP framework is the ordering of frequencies. We build on the idea in [1], which relates total variation and shift in graph SP. Here we need an extension to our multiple-shift setting. To do so we first denote the set of generating shifts (meet-irreducible elements) as $\mathcal{G} = \{g_1, \dots, g_k\} \subset \mathcal{L}$.

Definition 1. We define the total variation of a signal \mathbf{s} w.r.t. a given shift $g \in \mathcal{G}$ as

$$\text{TV}_g(\mathbf{s}) = \|\mathbf{s} - T_g \mathbf{s}\|_2.$$

Further, we define the total variation as the k -tuple of the individual TV_g :

$$\text{TV}(\mathbf{s}) = (\text{TV}_g(\mathbf{s}))_{g \in \mathcal{G}}.$$

Since for applications it is convenient to only have one number, we also define the sum total variation as

$$\text{STV}(\mathbf{s}) = \sum_{g \in \mathcal{G}} \text{TV}_g(\mathbf{s}).$$

Theorem 1. The total variation of the Fourier basis vector \mathbf{f}^y , $y \in \mathcal{L}$, when normalized to $\|\mathbf{f}^y\|_2 = 1$, is given by the k -tuple

$$\text{TV}(\mathbf{f}^y) = (\iota_{y \not\leq g})_{g \in \mathcal{G}} \quad (6)$$

and thus

$$\text{STV}(\mathbf{f}^y) = |\{g \in \mathcal{G} \mid y \not\leq g\}|.$$

In particular

$$0 \leq \text{STV}(\mathbf{f}^y) \leq |\mathcal{G}| = k.$$

Further, the set of total variations $\mathcal{T} = \{\text{TV}(\mathbf{f}^y) \mid y \in \mathcal{L}\}$ is a poset w.r.t. componentwise comparison and isomorphic to \mathcal{L} : for $x, y \in \mathcal{L}$,

$$x \leq y \text{ if and only if } \text{TV}(\mathbf{f}^x) \leq \text{TV}(\mathbf{f}^y), \quad (7)$$

which means the frequencies inherit the partial order of \mathcal{L} . In particular, the lowest frequency is \mathbf{f}^{\min} with $\text{TV}(\mathbf{f}^{\min}) = (0, \dots, 0)$. STV yields a topological sorting of TV.

Proof. $\text{TV}_g(\mathbf{f}^y) = \|\mathbf{f}^y - T_g \mathbf{f}^y\|_2$. Using (4), this yields 1 if $y \not\leq g$ and 0 else, which proves (6).

For (7) let $x \leq y$ and let $g \in \mathcal{G}$. Then $y \leq g$ implies $x \leq g$, i.e., $x \not\leq g$ implies $y \not\leq g$, which yields $\text{TV}_g(\mathbf{f}^x) = (\iota_{x \not\leq g})_{g \in \mathcal{G}} \leq (\iota_{y \not\leq g})_{g \in \mathcal{G}} = \text{TV}_g(\mathbf{f}^y)$.

For the converse we first note that every element in $y \in \mathcal{L}$ can be written as the meet of $g \in \mathcal{G}$, which are necessary those larger than y : $y = \bigwedge_{g \in \mathcal{G}, y \leq g} g = y$. Since $\text{TV}(\mathbf{f}^x) \leq \text{TV}(\mathbf{f}^y)$ means that $y \leq g$ implies $x \leq g$, we obtain $x \leq y$ as desired. \square

The above definitions, frequency ordering, and total variations stay the same if the 2-norm is replaced by any p -norm, $1 \leq p < \infty$.

The total variation tuples in (6) consist of 1s and 0s only. Thus, Theorem 1 can be used to encode the elements of \mathcal{L} as bit vectors of length $|\mathcal{G}|$.

Fourier transform. We denote the spectrum (Fourier coefficients) of a signal \mathbf{s} as $\hat{\mathbf{s}} = (\hat{s}_y)_{y \in \mathcal{L}}$. Equation (3) shows that the inverse Fourier transform is given by

$$s_x = \sum_{y \in \mathcal{L}} (\iota_{y \leq x}) \hat{s}_y = \sum_{y \leq x} \hat{s}_y, \quad x \in \mathcal{L}. \quad (8)$$

This equation is inverted using the classical Moebius inversion formula (see [28, Sec. 3]) and yields the associated Fourier transform that we call *discrete lattice transform* (DLT or $\text{DLT}_{\mathcal{L}}$):

$$\hat{s}_y = \sum_{x \leq y} \mu(x, y) s_x. \quad (9)$$

Here, μ is the Moebius function, defined recursively as

$$\begin{aligned} \mu(x, x) &= 1, & \text{for } x \in \mathcal{L}, \\ \mu(x, y) &= - \sum_{x \leq z < y} \mu(x, z), & x \neq y. \end{aligned}$$

In matrix form,

$$\hat{\mathbf{s}} = \text{DLT}_{\mathcal{L}} \mathbf{s}, \quad \text{with } \text{DLT}_{\mathcal{L}} = [\mu(x, y) \mathbf{1}_{x \leq y}]_{y, x \in \mathcal{L}}.$$

Inverse frequency response. The spectrum $\hat{\mathbf{s}}$ in (9) and the frequency response $\bar{\mathbf{h}}$ in (5) are computed differently. However, (5) is similar to the inverse DLT in (8) and thus can also be inverted using the Moebius inversion formula, which now takes the form (see [28, Sec. 3, Cor. 3])

$$h_x = \sum_{y \geq x} \mu(x, y) \bar{h}_y, \quad x \in \mathcal{L}. \quad (10)$$

Since it is invertible, every frequency response can be realized by a suitably chosen filter. In particular, the trivial filter exists that leaves every signal unchanged, i.e., with $\bar{h}_y = 1$ for all $y \in \mathcal{L}$. In other words, there is a linear combination of the T_a , $a \in \mathcal{L}$ that is the identity matrix. If \mathcal{L} has a unique maximum \max , then the trivial filter is T_{\max} .

Convolution theorem. The preceding results yield the following convolution theorem:

$$\widehat{\mathbf{h} * \mathbf{s}} = \bar{\mathbf{h}} \odot \hat{\mathbf{s}},$$

where \odot denotes pointwise multiplication.

Fast algorithms. Fourier transform and frequency response and their inverses can be computed in $O(kn)$ many operation where $k = |\mathcal{G}|$ [29], [30]. In some cases this can be further improved to $O(|\mathcal{E}|)$, where $|\mathcal{E}|$ is the number of covering pairs.

Summary and join-semilattices. For convenience we collect the main concepts of DLSP in Table I together with the dual framework for join-semilattices whose derivation is completely analogous. The two are not fundamentally different but are transposes of each other in the following sense. Every meet-semilattice can be converted into a join-semilattice by inverting the order relation, i.e., the arrows in the cover graph. Meet-irreducible element become join-irreducible this way, and the shift matrices of the latter are transposes of those of the former. As a result, as Table I shows, the Fourier transform matrices and frequency response matrices are also transposes of each other.

The only major difference is in the frequency ordering, which in the case of a join-semilattice is inverted. This means $x \leq y$ implies that $\text{TV}(\mathbf{f}^x) \geq \text{TV}(\mathbf{f}^y)$. In particular, \mathbf{f}^{\max} is the lowest frequency, which makes sense since it is the constant, all-one vector.

IV. EXAMPLE

In this section we illustrate and instantiate the DLSP concepts using the small lattice previously shown in Fig. 1a.

Lattice signal. A lattice signal is shown in Fig 2a. It associates a real number s_x with every lattice element x .

Generating shifts. As mentioned before, the lattice is generated by five shifts: $\mathcal{G} = \{h, e, f, g, c\}$. For example shifting by e maps

$$\mathbf{s} \mapsto T_e \mathbf{s} = (s_{x \wedge e})_{x \in \mathcal{L}} = (s_a, s_b, s_a, s_a, s_e, s_b, s_a, s_e)^T, \quad \text{i.e., } T_e \text{ is the matrix}$$

$$T_e = \begin{bmatrix} 1 & 0 & 0 & 0 & 0 & 0 & 0 & 0 \\ 0 & 1 & 0 & 0 & 0 & 0 & 0 & 0 \\ 1 & 0 & 0 & 0 & 0 & 0 & 0 & 0 \\ 1 & 0 & 0 & 0 & 0 & 0 & 0 & 0 \\ 0 & 0 & 0 & 0 & 1 & 0 & 0 & 0 \\ 0 & 1 & 0 & 0 & 0 & 0 & 0 & 0 \\ 1 & 0 & 0 & 0 & 0 & 0 & 0 & 0 \\ 0 & 0 & 0 & 0 & 1 & 0 & 0 & 0 \end{bmatrix}.$$

Note that the number of generating shifts $|\mathcal{G}|$ appears large compared to $|\mathcal{L}|$. This is due to the small scale of the example. In the subset lattice (Fig. 1c), $|\mathcal{G}| = \log_2(|\mathcal{L}|)$.

Filters and convolution. A generic filter is given by $\mathbf{h} = (h_a)_{a \in \mathcal{L}}$. First we identify the trivial filter T with $T\mathbf{s} = \mathbf{s}$ for all \mathbf{s} , i.e., with a constant-one frequency response. Using (10) with $\bar{h}_y = 1$ for all $y \in \mathcal{L}$, we get

$$T = T_g + T_h - T_d.$$

As an example filter, we use what one might expect (and we will confirm below) as a basic low-pass filter (analogous to $h(z) = 1 + z_1^{-1} + z_2^{-1}$ in the z -domain for two-dimensional SP) that sums the trivial filter and all generating shifts (see Fig. 2b)

$$T + \sum_{g \in \mathcal{G}} T_g = 2T_h + 2T_g + T_f + T_e - T_d + T_c, \quad (11)$$

i.e.,

$$\mathbf{h} = (0, 0, 1, -1, 1, 1, 2, 2)^T. \quad (12)$$

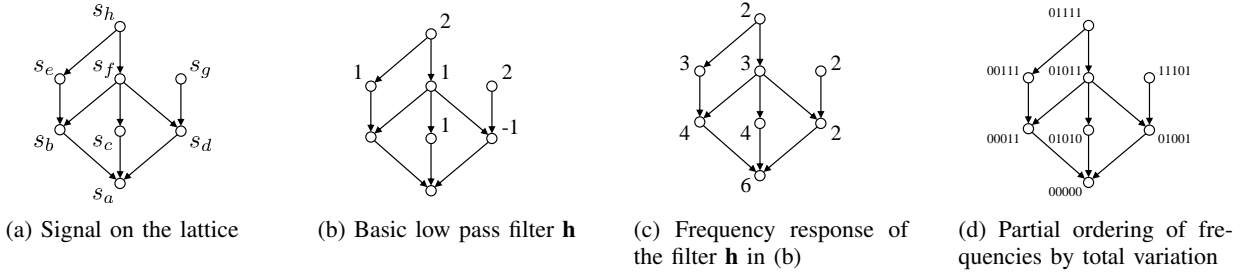
Fourier basis and frequency response. The Fourier basis vectors are computed with (3) and are indexed again by $y \in \mathcal{L}$. Collected in a matrix using the previous ordering of $y \in \mathcal{L}$, they take the form

$$\begin{bmatrix} 1 & 0 & 0 & 0 & 0 & 0 & 0 & 0 \\ 1 & 1 & 0 & 0 & 0 & 0 & 0 & 0 \\ 1 & 0 & 1 & 0 & 0 & 0 & 0 & 0 \\ 1 & 0 & 0 & 1 & 0 & 0 & 0 & 0 \\ 1 & 1 & 0 & 0 & 1 & 0 & 0 & 0 \\ 1 & 1 & 1 & 1 & 0 & 1 & 0 & 0 \\ 1 & 0 & 0 & 1 & 0 & 0 & 1 & 0 \\ 1 & 1 & 1 & 1 & 1 & 1 & 0 & 1 \end{bmatrix} \quad (13)$$

The frequency response of \mathbf{h} in (12) is computed with (5). For the filter in (12), the result is shown in Fig. 2c. We observe that lower frequencies are attenuated, so indeed \mathbf{h} is a low-pass filter. We note that the filter would

Concept	Meet-semilattice	Join-semilattice
Shift by $q \in \mathcal{L}$	$(s_x \wedge q)_{x \in \mathcal{L}}$	$(s_x \vee q)_{x \in \mathcal{L}}$
Generating shifts	meet-irr. $q \in \mathcal{L}$	join-irr. $q \in \mathcal{L}$
Convolution	$\sum_{q \in \mathcal{L}} h_q s_{x \wedge q}$	$\sum_{q \in \mathcal{L}} h_q s_{x \vee q}$
DLT $\hat{s}_y =$	$\sum_{x \leq y} \mu(x, y) s_x$	$\sum_{x \geq y} \mu(y, x) s_x$
Inverse DLT $s_x =$	$\sum_{y \leq x} \hat{s}_y$	$\sum_{y \geq x} \hat{s}_y$
Frequency resp. $\bar{h}_y =$	$\sum_{x \geq y} h_x$	$\sum_{x \leq y} h_x$
Inverse frequency resp. $h_x =$	$\sum_{y \geq x} \mu(x, y) \bar{h}_y$	$\sum_{y \leq x} \mu(y, x) \bar{h}_y$
Total variation	$\text{TV}(\mathbf{f}^y) = (\iota_{y \not\leq g})_{g \in \mathcal{G}}$	$\text{TV}(\mathbf{f}^y) = (\iota_{y \not\geq g})_{g \in \mathcal{G}}$
Frequency ordering	$x \leq y \Leftrightarrow \text{TV}(\mathbf{f}^x) \leq \text{TV}(\mathbf{f}^y)$	$x \leq y \Leftrightarrow \text{TV}(\mathbf{f}^x) \geq \text{TV}(\mathbf{f}^y)$
Lowest frequency	$\mathbf{f}^{\min} = (1, \dots, 1)^T$	$\mathbf{f}^{\max} = (1, \dots, 1)^T$

TABLE I: Basic DLSP concepts for meet- and join-semilattices.

Fig. 2: Basic concepts for the example lattice \mathcal{L} in Fig. 1a.

also be low-pass if T in (11) is omitted or if only a subset of the coefficients $h_g, g \in \mathcal{G}$ would be set to 1.

Frequency ordering. The total variation is a five-tuple for this case, one element per generator $\in \mathcal{G}$. As explained these five-tuples form a lattice isomorphic to \mathcal{L} , shown in Fig. 2d, partially ordered by componentwise comparison of five-tuples. Smaller elements have a lower sum total variation, the smallest is 0 for the constant Fourier basis vector $\mathbf{f}^a = \mathbf{f}^{\min}$.

Fourier transform. The DLT in matrix form is obtained via the Moebius inversion formula (9) or by inverting the matrix in (13):

$$\text{DLT}_{\mathcal{L}} = \begin{bmatrix} 1 & 0 & 0 & 0 & 0 & 0 & 0 & 0 \\ -1 & 1 & 0 & 0 & 0 & 0 & 0 & 0 \\ -1 & 0 & 1 & 0 & 0 & 0 & 0 & 0 \\ -1 & 0 & 0 & 1 & 0 & 0 & 0 & 0 \\ 0 & -1 & 0 & 0 & 1 & 0 & 0 & 0 \\ 2 & -1 & -1 & -1 & 0 & 1 & 0 & 0 \\ 0 & 0 & 0 & -1 & 0 & 0 & 1 & 0 \\ 0 & 1 & 0 & 0 & -1 & -1 & 0 & 1 \end{bmatrix} \quad (14)$$

It diagonalizes the (matrix representation) of every filter and every shift. For example

$$\text{DLT}_{\mathcal{L}} \cdot T_e \cdot \text{DLT}_{\mathcal{L}}^{-1} = \text{diag}(1, 1, 0, 0, 1, 0, 0, 0).$$

and for the low-pass filter \mathbf{h} in (12),

$$\text{DLT}_{\mathcal{L}} \cdot \left(\sum_{a \in \mathcal{L}} h_a T_a \right) \cdot \text{DLT}_{\mathcal{L}}^{-1} = \text{diag}(6, 4, 4, 2, 3, 3, 2, 2).$$

V. PROPERTIES AND RELATION TO GSP

We briefly summarize salient properties of DLSP and discuss the difference to GSP.

Properties. DLSP is combinatorial in nature in that it captures the partial order structure of the index domain. The combinatorial structure shows in the pure frequencies and their total variations, which both consists of 0 and 1 entries only.

The DLT is triangular and thus not orthogonal, so no Parseval identity holds in DLSP. This is not uncommon in SP where so-called biorthogonal transforms have been studied and used in the literature.

A meet-semilattice does not have a unique maximum in general. There are two arguments for adding an artificial such maximum. First, adding such an element (if not yet available) makes \mathcal{L} a lattice, i.e., a simultaneous meet- and join-semilattice. This means that two types of shifts, and thus convolutions, and DLTs are then available. Mixing these into one is nontrivial and a possible topic for future research. In particular, meet- and join-shifts cannot be diagonalized simultaneously since they do not commute. Second, if \mathcal{L} contains a unique maximum \max , the trivial filter is simply given by T_{\max} , which is the identity matrix.

It is intriguing that DLSP provides a *partial* ordering of frequencies. However, the same occurs in two-dimensional separable SP based on the separable DFT. Applied to an image, for example, yields a two-

dimensional array of frequencies that can also be viewed as partially ordered.

Note that the Fourier transform and frequency response are calculated differently. This is not surprising as they have different algebraic roles [9] and this also happens in graph SP.

Difference to GSP. DLSP is different from graph SP in two fundamental ways. First, DLSP is based on not one but several basic (generating) shifts that are needed to generate the filter algebra. In fact, every linear SP framework based on one generating shift can be viewed as a form of graph SP [10, p. 56] and vice-versa. Second, lattices, if represented as graph, constitute the very special subclass of directed acyclic graphs that correspond to a meet- or join-semilattice. The shift operation does not capture the adjacency structure of this graph but the partial order structure. E.g., $h \wedge g = a$ in our example lattice in Fig. 1a where a is several graph hops away from both g and h . Note that directed acyclic graphs are troublesome in graph SP since the adjacency matrix has only the eigenvalue 0 (assuming no self-loops) and is not (or rather far from) diagonalizable with large Jordan blocks.

Other related work. Lattice theory [26] is well-developed but does not discuss convolution or Fourier analysis. Fast Fourier transforms on groups and other algebraic structures are a classical topic in computer science, and there most closely related our work is [29] (and some of the references therein). The authors derive fast lattice Fourier transform algorithms, in the sense introduced here, but not a complete SP framework.

The simplicial complexes considered as index domain in [6] are meet-semilattices but possess additional topological structure that the authors use to define an SP framework very different from ours.

We show later in Section VII that DLSP can be applied to hypergraphs, but in a way different from the tensor-based approach in [4].

The powerset is a lattice with a hypercube as cover graph. Powerset signals, usually called set functions, have a rich set of applications in machine learning and beyond [31]. We introduced an SP framework for set functions in [8], part of which can be seen as special case of this paper. However, the special structure of powersets provide additional shifts (namely, the set difference has no generalization to lattices) and thus SP frameworks and an interpretation as so-called coverage functions.

Finally, [32] used the lattice convolution from our preliminary [23] to define lattice neural networks.

VI. SUBSET LATTICES

The power set 2^N of a finite set N forms a lattice with meet \cap and join \cup and its cover graph is a hypercube (e.g., Fig. 1c). Signals on the powerset lattice are called

set functions and the special structure of the lattice gives Fourier basis and Fourier transform a very regular structure and yields additional properties [8].

Any subset of the powerset lattice that is closed under \cap is a meet-semilattice. In the following we show that the reverse is also true, i.e., every meet-semilattice can be viewed as a subset lattice with \cap as meet. For example, Fig. 1b is isomorphic to $\{a, c, f, h\}$ in Fig. 1c. This is relevant since it enables the encoding of lattice elements, viewed as subsets, as bit vectors with bitwise and as the meet operation. Further, it shows that lattice signals can be viewed as sparse set functions.

Let \mathcal{L} be a meet-semilattice. If \mathcal{L} does not contain a unique maximum, we add one $\mathcal{L}' = \mathcal{L} \cup \{\max\}$ to obtain a lattice (Lemma 1). In \mathcal{L}' we let \mathcal{G} be the set of join-irreducible elements. Note that $\max \notin \mathcal{G}$ since otherwise it would cover only one element which would then already be a unique maximum in \mathcal{L} . Thus, $\mathcal{G} \subseteq \mathcal{L}$. With this we can express \mathcal{L} isomorphically as a subset lattice:

Theorem 2. *The mapping*

$$\phi : \mathcal{L} \rightarrow 2^{\mathcal{G}}, \quad x \mapsto \{g \in \mathcal{G} \mid g \leq x\}$$

satisfies

$$\phi(x \wedge y) = \phi(x) \cap \phi(y).$$

Proof. $\phi(x \wedge y) = \{g \in \mathcal{G} \mid g \leq x \wedge y\} = \{g \in \mathcal{G} \mid g \leq x \text{ and } g \leq y\} = \phi(x) \cap \phi(y)$. \square

The analogous construction for a join-semilattice yields an isomorphism that satisfies $\phi(x \vee y) = \phi(x) \cup \phi(y)$.

For the lattice in Fig. 1a, we obtain the join-irreducibles $\mathcal{G} = \{b, c, d, e, g\}$ and thus \mathcal{L} is isomorphic to a subset lattice of a powerset lattice with five elements.

The construction in Theorem 2 was also used in [29] to obtained fast lattice Fourier transforms.

VII. APPLICATION EXAMPLE: FORMAL CONCEPT LATTICES IN SOCIAL DATA ANALYSIS

In this section we present one possible application domain for DLSP: the well-developed area of formal concept lattices (FCLs) used in social data analysis [14]. These lattices can be seen as a compressed representation of relations between objects and attributes. Equivalently such a relation can be viewed as a bipartite graph or a hypergraph. DLSP provides a notion of filtering and Fourier analysis for data on these relations.

We first explain FCLs using a small example and then consider a larger data set on information about customers of a telecommunication company.

A small motivating example. Table II shows a sample of seven customers (users) of a telecommunication

Property	User						
	U_1	U_2	U_3	U_4	U_5	U_6	U_7
P_1 : Gender		×		×	×		
P_2 : Partner	×			×	×	×	×
P_3 : Dependents				×	×	×	×
P_4 : InternetService	×	×	×		×		×
P_5 : DeviceProtection		×			×		
P_6 : TechSupport							×
P_7 : StreamingMovies		×			×		
P_8 : PaperlessBilling	×	×	×		×		

TABLE II: A sample of the telecommunications data set.

service with eight binary properties². For example, user U_3 has internet service and prefers paperless billing.

Every user satisfies a number of properties and every property is satisfied by a certain number of users. This relationship can be extended to sets of users and sets of properties. For example properties $\{P_1, P_2\}$ are satisfied by the users $\{U_4, U_5\}$. Conversely, the properties jointly satisfied by $\{U_4, U_5\}$ also include P_3 : $\{P_1, P_2, P_3\}$, so this relationship between sets of users and sets of properties is not always one-to-one. For $\{U_4, U_5\}$ and $\{P_1, P_2, P_3\}$ it is and defines a so-called formal concept.

More specifically, a formal concept is a pair of objects (here: users) and attributes (here: properties) such that the objects are specified by the attributes and vice versa. In Table II each formal concept corresponds to a maximal rectangles of crosses.

The formal concepts form the FCL, which for Table II is shown in Fig. 3, using a shorthand notation for sets. The formal concepts are partially ordered by inclusion of object sets, or, equivalently, by inverse inclusion of attribute sets (more objects mean fewer attributes are satisfied). The meet is obtained by intersecting attribute sets and the join by intersecting object sets.

For example, the minimal element $(U_{12\dots7}, \emptyset)$ shows that no property is satisfied by all users and vice-versa. The aforementioned (U_{45}, P_{123}) is a lattice element. The meet of (U_7, P_{2346}) and (U_{45}, P_{123}) is obtained by intersecting the property sets and yields (U_{14567}, P_2) .

Finally, we note that the original table can be reconstructed from the FCL, since every \times is contained in at least one concept.

Formal concept lattice. We now more formally define formal concept lattices. Let \mathcal{O} be a finite set of objects and \mathcal{A} a finite set of attributes. Let $\mathcal{R} \subseteq \mathcal{O} \times \mathcal{A}$ be a binary relation with $(o, a) \in \mathcal{R}$ iff object o has attribute a . For $O \subseteq \mathcal{O}$ and $A \subseteq \mathcal{A}$, let

$$\text{attr}(O) = \{a \in \mathcal{A} \mid (o, a) \in \mathcal{R} \text{ for all } o \in O\}$$

²The data is part of the IBM sample data sets https://www.ibm.com/support/knowledgecenter/SSEP7J_11.1.0/com.ibm.swg.ba.cognos.ig_smpls.doc/c_telco_dm_sam.html. The data set is available under <https://www.kaggle.com/blastchar/telco-customer-churn>

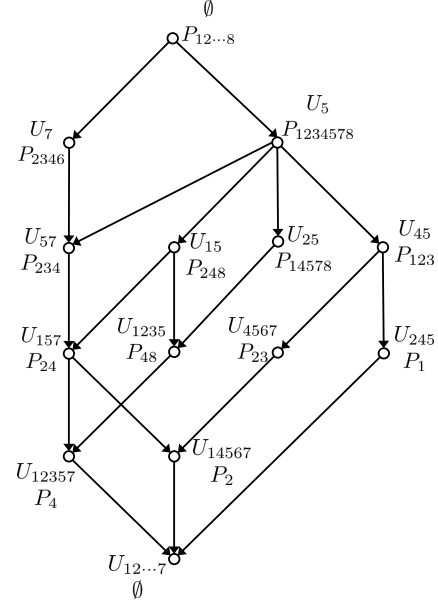


Fig. 3: The formal concept lattice, with 14 elements, of the data set in Table II. We use the shorthand notations $P_{k_1, \dots, k_j} = \{P_{k_1}, \dots, P_{k_j}\}$ and $U_{k_1, \dots, k_j} = \{U_{k_1}, \dots, U_{k_j}\}$.

be the set of joint attributes of the objects in Q , and let

$$\text{obj}(A) = \{o \in O \mid (o, a) \in I \text{ for all } a \in B\}$$

be the set of objects that satisfy all attributes in B .

A pair $(O, A) \in 2^{\mathcal{O}} \times 2^{\mathcal{A}}$ is called a *formal concept* if $\text{attr}(O) = A$ and $\text{obj}(A) = O$. In a relation table like Table II these corresponds to the maximal rectangles of crosses.

The formal concepts induced by the relation \mathcal{R} form a lattice with partial order $(O_1, A_1) \leq (O_2, A_2)$ iff $A_1 \subseteq A_2$ (or equivalently iff $O_2 \subseteq O_1$). The meet operation is given by

$$(O_1, A_1) \wedge (O_2, A_2) = (\text{obj}(\text{attr}(O_1 \cup O_2)), A_1 \cap A_2), \quad (15)$$

i.e., by intersecting attributes and collecting the associated objects. In the relation table it corresponds to the maximal subrectangle of the two initial rectangles.

Analogously, the join is given by

$$(O_1, A_1) \vee (O_2, A_2) = (O_1 \cap O_2, \text{attr}(\text{obj}(A_1 \cup A_2))). \quad (16)$$

We note that, in a dual way, the FCL can be defined to be upside down, i.e., with inverted order and flipped meet/join definitions. We also note that every lattice is isomorphic to a suitable FCL [33, Thm. 1].

Formal concept data. Assume that we have further data on the users, e.g., in our previous example, whether they have canceled their contract (so-called churn variable, 0 or 1) and we want to understand the mapping from user properties to the churn. It is then natural to first collect users defined by the same properties (since they are indistinguishable) into sets as done by the FCL, and average the churn (between 0 and 1) over these sets, which yields a lattice signal.

As a prototypical example, we expand our previous example by selecting 11 binary properties and all 7043 customers from the telecommunication data set. Using the Python library *Concepts*³ we calculate the associated FCL, which has 813 elements. As lattice signal we use the average on the aforementioned churn variable for a user set in a concept, but subtract the average churn over all users. So the signal captures the deviation from the average churn, which is 0.2654, for every concept.

The signal and its meet and join Fourier transforms are shown in Fig. 4. For example, the value at the maximum of the signal is -0.0654 and corresponds to the set of ten customers that satisfy all properties. The value at the minimum is zero and corresponds to the set of all customers that satisfy the empty set of properties.

We observe that the meet and join spectrum are fundamentally different but in both cases the signal is in tendency low frequency, more pronounced for the meet DLT. Further, the spectra reveal structure. They are approximately sparse and high values show transitions between property sets that are relevant for the churn variable. Building on DLSP one can imagine porting now basic SP methods for compression, sampling, or completion to social data analysis this way and also work on developing a deeper understanding on meaning of spectrum. Doing so is outside the scope of this paper, as we also wish to present another application domain in the next section.

Relation to bipartite graphs and hypergraphs. The relation \mathcal{R} defines an undirected bipartite graph with nodes $\mathcal{O} \cup \mathcal{A}$ and an edge between two nodes if $(o, a) \in \mathcal{R}$. Conversely, every bipartite graph defines a relation this way. \mathcal{R} also defines a hypergraph with nodes \mathcal{O} and hyperedges $\text{attr}(a), a \in \mathcal{A}$ or nodes \mathcal{A} and hyperedges $\text{obj}(o), o \in \mathcal{O}$. Conversely, every hypergraph defines a relation this way. Thus, DLSP via FCLs, offers a form of Fourier analysis for these index domains, different from graph SP in [1] or hypergraph SP in [4].

VIII. APPLICATION EXAMPLE: MULTISSET LATTICES IN SPECTRUM AUCTIONS

As a second prototypical application example we consider spectrum auctions. We first show that bidders'

preferences, called value functions, in such auctions can be modeled as signals on multiset lattices. Then we state a sampling theorem for DLSP and apply it to reconstruct these value functions from few samples. Finally, we port Wiener filtering to DLSP and use it to remove white noise from value functions.

A. Multiset lattices

We first introduce lattices and then explain how signals on such lattices naturally appear as value functions in spectrum auctions.

Lattice. A multiset is a generalization of a set that allows an element to appear more than one time. Assuming a ground set $\{x_1, \dots, x_f\}$ of f available elements, each (finite) multiset can be represented by a vector $m = (m_1, \dots, m_f) \in \mathbb{N}_0^f$, where each m_i specifies how often elements i occurs in the set. For example, $(2, 1)$ represents $\{x_1, x_1, x_2\}$. A multiset m is a set if all $m_i \leq 1$, i.e., is a bit vector, a common representation for sets.

A multiset a is a submultiset of m if $a \leq m$, defined componentwise. The set of submultisets $\mathcal{L} = \{a \in \mathbb{N}_0^f : a \leq m\}$ of a given multiset m is a lattice with meet $a \wedge b = \min(a, b)$ and join $a \vee b = \max(a, b)$, for $a, b \in \mathcal{L}$, where the minimum and maximum is taken componentwise. The multiset lattice \mathcal{L} has $|\mathcal{L}| = \prod_{1 \leq i \leq f} (m_i + 1)$ elements. A special case is the powerset lattice, for which $m_i = 1$ for all i . Note that if elements of a set are exchangeable, the multiset lattice has fewer elements than the powerset lattice, cf. Fig. 5.

Spectrum auctions. Spectrum auctions [34] are combinatorial auctions [35] in which licenses for bands of the electromagnetic spectrum are sold to bidders, e.g., telecommunication companies. For some bands there are multiple equal licenses, which makes the set of available licenses a multiset m .

Lattice signal. Each bidder in such an auction is modeled as value function that assigns to each submultiset a of available licenses a nonnegative value s_a . The value function is thus a multiset signal $\mathbf{s} = (s_a)_{a \in \mathcal{L}}$, where \mathcal{L} is the lattice of submultisets of m as explained below.

To find an allocation of the licenses to the bidders, an auctioneer first elicits the bidders' preferences by asking values s_a for a small number of $a \in \mathcal{L}$, since the complete \mathbf{s} is too large or too expensive to obtain. In other words, the auctioneer samples the \mathbf{s} and an important problem is how to do this well [36].

As usual in the research on spectrum auctions, we consider simulated bidders. In particular, here we use the single region value model (SRVM) from the spectrum auctions test suite (SATS) [37]. SATS allows us to create multiple auction instances, and each instance comes with its own set of bidders. There are four different bidder types: small, high-frequency, secondary, and primary

³Available online at <https://github.com/xflr6/concepts>.

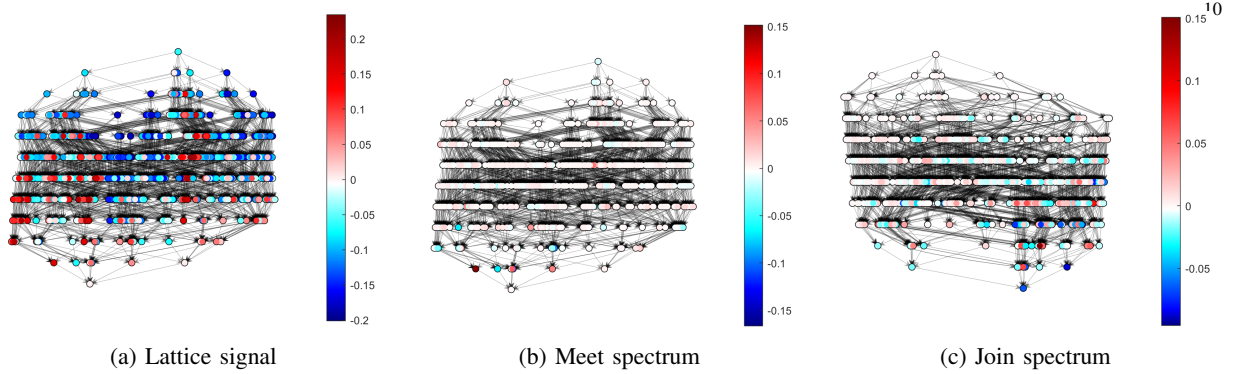


Fig. 4: The signal and its meet and join spectrum on the formal concept lattice of the data on the customers of a telecommunication company. Note that for the join spectrum, the lattice is inverted to have low frequencies on the bottom (see Table I).

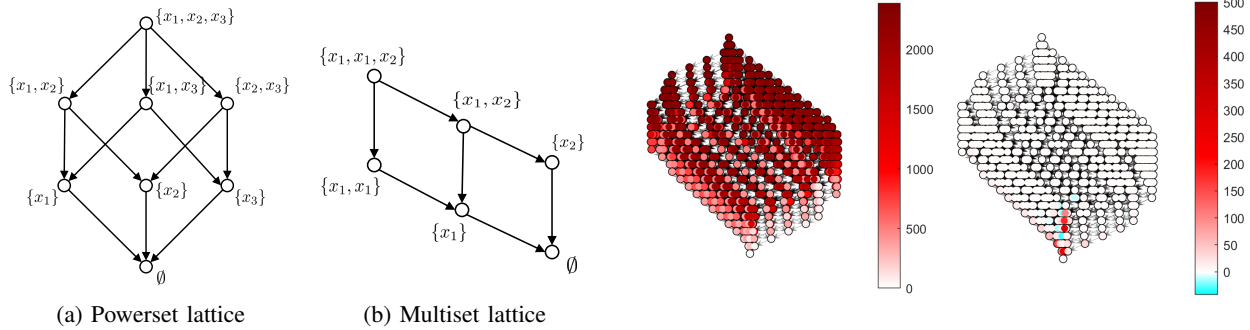


Fig. 5: If elements are exchangeable, e.g., if x_1 and x_3 are the same thing, the powerset lattice (a) requires more elements than the multiset lattice (b) to model the situation accurately.

Fig. 6: A secondary bidder as signal on a multiset lattice and its Fourier transform.

bidders. The bidders' value functions depend on its type, e.g., small bidders prefer submultisets with few licenses, high-frequency bidders prefer licenses for high-frequency bands, etc. In SRVM the multiset of all available licenses is $m = (6, 14, 9)$. Modeling SRVM bidders' value functions as multiset functions instead of the commonly used set functions [38], [39] thus reduces the dimensionality of value functions from $2^{6+14+9} = 2^{29}$ to $7 \cdot 15 \cdot 10 = 1050$.

In Fig. 6 we show one example of a value function for one secondary bidder in SRVM and its Fourier transform. Relatively few of the frequencies contribute to the overall signal, i.e., the signal is Fourier sparse. Thus, a proper sampling strategy could yield complete information on the signal with few samples. We introduce a sampling theorem next.

B. Sampling

In this subsection we extend DLSP with a sampling theorem, first presented in [24], for the perfect

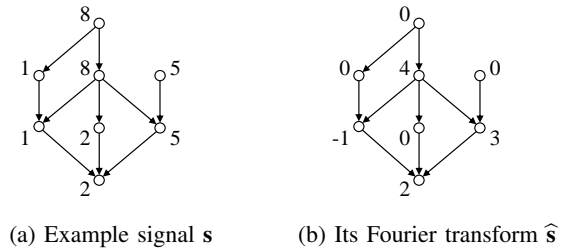


Fig. 7: A signal on \mathcal{L} in Fig. 1a, which is 4-sparse in the Fourier domain with support $\mathcal{B} = \{a, b, d, f\}$.

reconstruction of lattice signals that are sparse in the DLT Fourier domain, i.e., where only a subset of the frequencies has non-zero content.

In the following we call a lattice signal s k -Fourier-sparse if its Fourier support \mathcal{B} satisfies

$$|\text{supp}(\hat{s})| = |\mathcal{B}| = |\{b \in \mathcal{L} : \hat{s}_b \neq 0\}| = k. \quad (17)$$

As an example, the signal in Fig. 7 is 4-sparse. Following the general paradigm of classical sampling theory [40], we are looking for a linear sampling operator $P_{\mathcal{A}}$ that reduces the signal s to $|\mathcal{A}| = k = |\mathcal{B}|$ samples such that

$$\begin{aligned}
& \begin{bmatrix} 1 & 0 & 0 & 0 \\ 0 & 1 & 0 & 0 \\ 0 & 0 & 0 & 0 \\ 0 & 0 & 1 & 0 \\ 0 & 0 & 0 & 0 \\ 0 & 0 & 0 & 1 \\ 0 & 0 & 0 & 0 \\ 0 & 0 & 0 & 0 \end{bmatrix}^T \begin{bmatrix} 2 \\ 1 \\ 2 \\ 5 \\ 1 \\ 8 \\ 5 \\ 8 \end{bmatrix} = \begin{bmatrix} 2 \\ 1 \\ 5 \\ 8 \end{bmatrix} \quad (a) P_B \mathbf{s} = \mathbf{s}_B \\
& \begin{bmatrix} 1 & 0 & 0 & 0 \\ 0 & 1 & 0 & 0 \\ 1 & 0 & 0 & 0 \\ 0 & 0 & 1 & 0 \\ 0 & 1 & 0 & 0 \\ 0 & 0 & 0 & 1 \\ 0 & 0 & 1 & 0 \\ 0 & 0 & 0 & 1 \end{bmatrix} \begin{bmatrix} 2 \\ 1 \\ 5 \\ 8 \end{bmatrix} = \begin{bmatrix} 2 \\ 1 \\ 2 \\ 5 \\ 1 \\ 8 \\ 5 \\ 8 \end{bmatrix} \quad (b) \mathbf{s} = I_B \mathbf{s}_B
\end{aligned}$$

Fig. 8: (a) Sampling and (b) interpolation of the Fourier-sparse lattice signal shown in Fig. 7.

there exists a linear interpolation operator I_A that allows for perfect recovery of \mathbf{s} from these samples: $\mathbf{s} = I_A P_A \mathbf{s}$. The triangular shape of the Fourier transform makes this task easy.

Let $\mathcal{A} = \{a_1, \dots, a_k\} \subseteq \mathcal{L}$. We consider the associated sampling operator

$$P_A : \mathbb{R}^n \mapsto \mathbb{R}^k, \mathbf{s} \mapsto \mathbf{s}_A = (s_{a_1}, \dots, s_{a_k})^T. \quad (18)$$

Theorem 3 (Lattice sampling). *Let \mathbf{s} be a k -sparse lattice signal on \mathcal{L} with Fourier support \mathcal{B} . Then \mathbf{s} can be perfectly reconstructed from the samples $\mathbf{s}_B = P_B \mathbf{s}$.*

Namely, $\mathbf{s} = I_B \mathbf{s}_B$ with $I_B = \text{DLT}_{\mathcal{L}, \mathcal{B}}^{-1} (\text{DLT}_{\mathcal{B}, \mathcal{B}}^{-1})^{-1}$. The matrix $\text{DLT}_{\mathcal{A}, \mathcal{B}}^{-1}$ is the sub-matrix of DLT^{-1} obtained by selecting the rows indexed by \mathcal{A} and the columns indexed by \mathcal{B} .

Proof. As \mathbf{s} has Fourier support \mathcal{B} , we have

$$\mathbf{s} = \text{DLT}_{\mathcal{L}, \mathcal{B}}^{-1} \hat{\mathbf{s}}_B.$$

Applying the sampling operator P_B to both sides yields

$$\mathbf{s}_B = \text{DLT}_{\mathcal{B}, \mathcal{B}}^{-1} \hat{\mathbf{s}}_B.$$

What remains to show is that $\text{DLT}_{\mathcal{B}, \mathcal{B}}^{-1}$ is invertible. However, this is the case because of its triangular shape (when \mathcal{L} is topologically sorted) with 1s on the diagonal. \square

Fig. 8 instantiates Theorem 3 for the lattice in Fig. 7 to sample and reconstruct \mathbf{s} .

Experiment. Recently, several machine learning based preference elicitation [36] schemes, where the bidders' preferences are modeled by, e.g., neural networks [38], have been proposed. We sketch a similar prototypical preference elicitation scheme based on DLSP sampling, leveraging Fourier sparsity.

Our sampling theorem allows us to find a Fourier-sparse approximation of a value function if the Fourier support of the most important frequencies is known, which, in general is not the case. To overcome this issue, we compute the Fourier support from one auction instance of bidders and then use it for new auction instances and bidders, querying them according to Theorem 3.

We noted that in the SRVM model all bidders were Fourier-sparse with respect to the DLT and their support did not change between different auction instances. Thus we achieved perfect reconstruction from very few queries in all cases. We show our results in Table III.

	small	high-freq.	secondary	primary
Join-semilattice	20	48	60	60
Meet-semilattice	36	90	111	111

TABLE III: Number of non-zero Fourier coefficients (= number of queries) required for perfect reconstruction for different bidder types in SRVM.

C. Wiener filter with energy-preserving shift

in this section we port Wiener filtering to DLSP using SRVM bidders as a case study. Our approach follows closely the one taken in graph SP by [41]. Namely, we first define an energy-preserving shift on which the Wiener filter is built. Part of this subsection are submitted in [42].

Energy-preserving shift. The lattice shifts, just as the graph shift, are not energy-preserving. Thus, similar to [41] we first the energy-preserving lattice shift as

$$T_e = \text{DLT}^{-1} \cdot \Lambda_e \cdot \text{DLT} \quad (19)$$

with $\Lambda_e = \text{diag}(\exp(-2\pi j k / |\mathcal{L}|) \mid k = 0, \dots, |\mathcal{L}| - 1)$. The frequency response of T_e is the diagonal of Λ_e and hence T_e is a filter. The filter coefficients can be calculated using (10). We summarize its properties.

Theorem 4 (Properties of T_e). *The energy-preserving shift T_e in (19):*

- (i) $\|\text{DLT} \mathbf{s}\|_2 = \|\text{DLT}(T_e \mathbf{s})\|_2$, i.e., it preserves energy,
- (ii) every lattice filter is a polynomial in the energy-preserving shift.

Proof. Property (i) follows from the simple derivation

$$\begin{aligned}
\|\text{DLT}(T_e \mathbf{s})\|_2 &= \|\text{DLT} \text{DLT}^{-1} \Lambda_e \text{DLT} \mathbf{s}\| \\
&= \|\Lambda_e \text{DLT} \mathbf{s}\| = \|\text{DLT} \mathbf{s}\|_2,
\end{aligned}$$

in which the last equality holds because Λ_e is unitary.

For (ii) we need to find a polynomial p_H to a given filter H such that $p_H(T_e) = H$. Let $D_H = \text{DLT} H \text{DLT}^{-1}$ be the diagonal filter in the frequency domain. Thus, equivalently, we need to p_H with $p_H(\Lambda_e) = D_H$. This is possible since all diagonal elements of Λ_e are distinct and can be done, e.g., with Lagrange interpolation. \square

Note that unlike the generating shifts, the energy-preserving shift does not act locally, but is, in general, a full triangular matrix with complex entries.

Lattice Wiener filters. A Wiener filter is an optimal denoising filter designed from a noisy version of a known

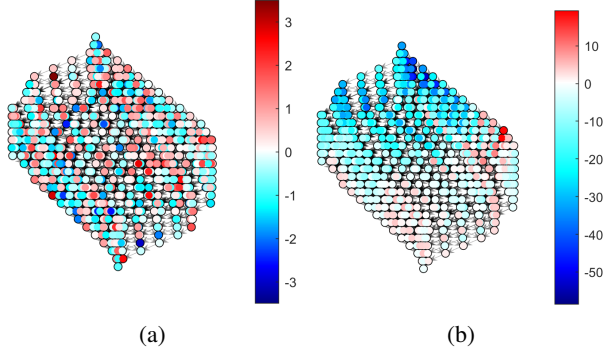


Fig. 9: White lattice noise in (a) frequency and (b) lattice domain.

reference signal. Such a filter can handle noisy signals, which are similar to the reference signal and where the noise is from the same noise model.

Consider a lattice signal \mathbf{s} and a noisy measurement of the signal $\mathbf{y} = \mathbf{s} + \mathbf{n}$. The lattice Wiener filter of order N based on the energy-preserving shift has then the form

$$H = \sum_{k=0}^N h_k T_e^k, \quad (20)$$

where the filter coefficients \mathbf{h} can be found by minimizing the Euclidean error

$$\min_{\mathbf{h}} \|\mathbf{H}\mathbf{y} - \mathbf{s}\|_2^2. \quad (21)$$

We can rewrite (21) as

$$\min_{\mathbf{h}} \|\mathbf{B}\mathbf{h} - \mathbf{s}\|_2^2, \quad \text{with } \mathbf{B} = [\mathbf{y} \ T_e \mathbf{y} \ \dots \ T_e^{L-1} \mathbf{y}]. \quad (22)$$

The solution of this minimization problem is given by the solution of the linear system

$$\mathbf{B}^H \mathbf{B} \mathbf{h} = \mathbf{B}^H \mathbf{s} \quad (23)$$

for the coefficients \mathbf{h} of the Wiener filter. Note that the powers of T_e can be computed efficiently in the frequency domain using $T_e^k = \text{DLT}^{-1} \Lambda_e^k \text{DLT}$.

Lattice white noise. White noise has equal intensity across frequencies. In settings where the Fourier transform is orthogonal (e.g., discrete time SP), white noise can be simulated by adding a Gaussian noise vector with independent components to the signal. The same procedure does not lead to white noise for a lattice signal, as the DLT is not orthogonal. Thus we always add white noise directly in the frequency domain. In Fig. 9 we show an examples of white noise in lattice and frequency domain.

Experimental setup. For the experiment we used one secondary bidder as reference signal \mathbf{s}^{ref} and one primary bidder as test signal \mathbf{s}^{test} . We added (different) white lattice noise to the reference and test signal leading to a

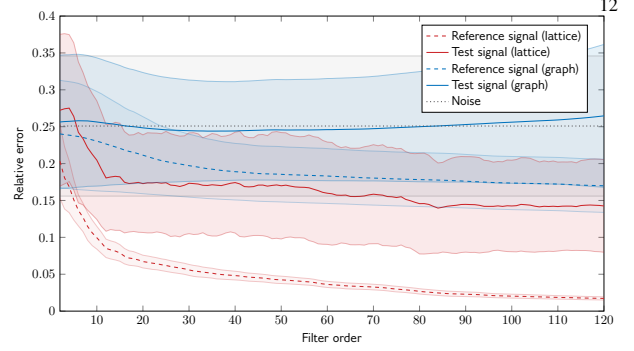


Fig. 10: Denoising a bidder signal with lattice (red) and graph Wiener filter (blue) of different order. The results on the reference signals in both cases are shown dashed. The shaded areas are the standard deviations over 100 simulations.

signal-to-noise ratio of 12.5 ± 2.5 dB. We repeated the experiment with 100 noise samples to obtain the standard deviation.

Benchmark. As benchmark we compare the lattice Wiener filter to a graph Wiener filter based on the cover graph as constructed in [41]. Since the cover graph is directed and acyclic it is not diagonalizable as required by [41]. Thus we use instead the undirected cover graph. Note that the graph Wiener filter has the disadvantage that lattice white noise cannot be modulated with graph filters.

Results. Fig. 10 shows the relative reconstruction error as function of the filter order, for the lattice and graph Wiener filtered signal. The qualitative behavior on the reference signal for the graph Wiener filter is as expected from [41], but is outperformed by the lattice Wiener filter. On the test signal the graph Wiener filter raises the relative error, while the lattice Wiener filter reduces it.

IX. CONCLUSION

We presented discrete-lattice SP, a meaningful reinterpretation of fundamental SP concepts for signals indexed by partially ordered sets that support a meet (or join) operation. Lattices can be represented as cover graphs, but the lattice shifts operate very differently from graph shifts, capturing the partial order structure rather than proximity. Further, cover graphs are directed and acyclic and thus only have the eigenvalue zero, a problem in graph SP.

Lattices are a fundamental structure in many domains as indicated in the introduction. In this paper we could only consider two examples: multiset lattices and formal concept lattices. We see particular potential in the latter, since with these lattices DLSP provides a general and

novel form of Fourier analysis for data on relations, or, equivalently, bipartite graphs or hypergraphs.

Together with other novel SP frameworks that were recently introduced, DLSP shows how the power of traditional SP tools can be brought to new domains and to new kinds of data.

REFERENCES

- [1] A. Sandryhaila and J. M. F. Moura, "Discrete signal processing on graphs," *IEEE Trans. on Signal Processing*, vol. 61, no. 7, pp. 1644–1656, 2013.
- [2] D. Shuman, S. K. Narang, P. Frossard, A. Ortega, and P. Vandergheynst, "The emerging field of signal processing on graphs: Extending high-dimensional data analysis to networks and other irregular domains," *IEEE Signal processing Magazine*, vol. 30, no. 3, pp. 83–98, 2013.
- [3] A. Ortega, P. Frossard, J. Kovacevic, J. Moura, and P. Vandergheynst, "Graph Signal Processing: Overview, Challenges, and Applications," *Proc. IEEE*, vol. 106, no. 5, pp. 808–828, 2018.
- [4] S. Zhang, Z. Ding, and S. Cui, "Introducing hypergraph signal processing: Theoretical foundation and practical applications," *IEEE Internet of Things Journal*, vol. 7, no. 1, pp. 639–660, 2020.
- [5] L. Ruiz, L. F. O. Chamon, and A. Ribeiro, "Graphon signal processing," 2020.
- [6] S. Barbarossa and S. Sardellitti, "Topological signal processing over simplicial complexes," *IEEE Trans. on Signal Processing*, vol. 68, pp. 2992–3007, 2020.
- [7] A. Parada-Mayorga, H. Riess, A. Ribeiro, and R. Ghrist, "Quiver signal processing (qsp)," 2020.
- [8] M. Püschel and C. Wendler, "Discrete signal processing with set functions," 2020, submitted for publication.
- [9] M. Püschel and J. M. F. Moura, "Algebraic signal processing theory: Foundation and 1-D time," *IEEE Trans. on Signal Processing*, vol. 56, no. 8, pp. 3572–3585, 2008.
- [10] —, "Algebraic signal processing theory," *CoRR*, vol. abs/cs/0612077, 2006. [Online]. Available: <http://arxiv.org/abs/cs/0612077>
- [11] —, "Algebraic signal processing theory: 1-D space," *IEEE Trans. on Signal Processing*, vol. 56, no. 8, pp. 3586–3599, 2008.
- [12] A. Sandryhaila, J. Kovacevic, and M. Püschel, "Algebraic signal processing theory: 1-D nearest-neighbor models," *IEEE Trans. on Signal Processing*, vol. 60, no. 5, pp. 2247–2259, 2012.
- [13] M. Püschel and M. Rötteler, "Algebraic signal processing theory: 2-D hexagonal spatial lattice," *IEEE Trans. on Image Processing*, vol. 16, no. 6, pp. 1506–1521, 2007.
- [14] B. Ganter and R. Wille, *Formal Concept Analysis: Mathematical Foundations*. Springer Science & Business Media, 2012.
- [15] L. Wei and Q. Wan, "Granular transformation and irreducible element judgment theory based on pictorial diagrams," *IEEE Trans. on Cybernetics*, vol. 46, no. 2, pp. 380–387, 2016.
- [16] B. Monjardet and V. Raderanirina, "Lattices of choice functions and consensus problems," *Social Choice and Welfare*, no. 3, pp. 349–382, 23.
- [17] T. T. Lee, "An algebraic theory of relational databases," *The Bell Systems Technical Journal*, vol. 62, no. 10, pp. 3159–3204, 1983.
- [18] D. Klein, T. Ivanciuc, A. Ryzhov, and O. Ivanciuc, "Combinatorics of Reaction-Network Posets," *Combinatorial Chemistry & High Throughput Screening*, vol. 11, pp. 723–733, 2008.
- [19] P. Alberch, "From genes to phenotype: dynamical systems and evolvability," *Genetica*, vol. 84, no. 1, pp. 5–11, 1991.
- [20] N. Beerenwinkel, P. Knupfer, and A. Tresch, "Learning monotonic genotype-phenotype maps," *Statistical applications in genetics and molecular biology*, vol. 10, no. 1, 2011.
- [21] D. E. Bennett, R. J. Camacho, D. Otelea, D. R. Kuritzkes, H. Fleury, M. Kiuchi, W. Heneine, R. Kantor, M. R. Jordan, J. M. Schapiro *et al.*, "Drug resistance mutations for surveillance of transmitted hiv-1 drug-resistance: 2009 update," *PLoS one*, vol. 4, no. 3, p. e4724, 2009.
- [22] J.-C. Birget, "Partial orders on words, minimal elements of regular languages, and state complexity," *Theoretical Computer Science*, vol. 119, no. 2, pp. 267–291, 1993.
- [23] M. Püschel, "A Discrete Signal Processing Framework for Meet/Join Lattices with Applications to Hypergraphs and Trees," in *Proc. International Conference on Acoustics, Speech, and Signal Processing (ICASSP)*, 2019, pp. 5371–5375.
- [24] C. Wendler and M. Püschel, "Sampling signals on meet/join lattices," in *Proc. Global Conference on Signal and Information Processing (GlobalSIP)*, 2019, pp. 1–5.
- [25] R. P. Stanley, *Enumerative Combinatorics: Volume 1*, 2nd ed. Cambridge University Press, 2011.
- [26] G. Grätzer, *Lattice Theory: Foundation*. Birkhäuser, 2011.
- [27] M. Püschel, "A discrete signal processing framework for set functions," in *Proc. International Conference on Acoustics, Speech, and Signal Processing (ICASSP)*, 2018.
- [28] G.-C. Rota, "On the foundations of combinatorial theory. I. theory of Möbius functions," *Z. Wahrscheinlichkeitstheorie und Verwandte Gebiete*, vol. 2, no. 4, pp. 340–368, 1964.
- [29] A. Björklund, T. Husfeldt, P. Kaski, M. Koivisto, J. Nederlof, and P. Parviainen, "Fast zeta transforms for lattices with few irreducibles," *ACM Trans. on Algorithms*, vol. 12, no. 1, pp. 4:1–4:19, 2015.
- [30] P. Kaski, J. Kohonen, and T. Westerback, "Fast Möbius Inversion in Semimodular Lattices and ER-labelable Posets," *The Electronic Journal of Combinatorics*, vol. 23, no. 3, p. P3.26, 2016.
- [31] A. Krause and D. Golovin, *Tractability: Practical Approaches to Hard Problems*. Cambridge University Press, 2014, ch. Submodular function maximization, pp. 71–104.
- [32] H. Riess and J. Hansen, "Multidimensional Persistence Module Classification via Lattice-Theoretic Convolutions," 2020, arXiv preprint arXiv:2011.14057.
- [33] B. Ganter and R. Wille, "Applied lattice theory: Formal concept analysis," in *General Lattice Theory*, G. Grätzer, Ed. Birkhäuser, 1997.
- [34] P. Cramton, "Spectrum auction design," *Review of Industrial Organization*, vol. 42, no. 2, pp. 161–190, 2013.
- [35] L. M. Ausubel, P. Cramton, and P. Milgrom, "The clock-proxy auction: A practical combinatorial auction design," in *Combinatorial Auctions*. MIT Press, 2006, pp. 115–138.
- [36] T. Sandholm and C. Boutilier, "Preference elicitation in combinatorial auctions," *Combinatorial auctions*, vol. 10, 2006.
- [37] M. Weiss, B. Lubin, and S. Seuken, "Sats: A universal spectrum auction test suite," in *Proceedings of the 16th Conference on Autonomous Agents and MultiAgent Systems*, 2017, pp. 51–59.
- [38] J. Weissteiner and S. Seuken, "Deep learning-powered iterative combinatorial auctions," in *Proceedings of the 34th AAAI Conference of Artificial Intelligence*, 2020.
- [39] J. Weissteiner, C. Wendler, S. Seuken, B. Lubin, and M. Püschel, "Fourier Analysis-based Iterative Combinatorial Auctions," 2020, arXiv preprint arXiv:2009.10749.
- [40] M. Vetterli, J. Kovačević, and V. K. Goyal, *Foundations of signal processing*. Cambridge University Press, 2014.
- [41] A. Gavili and X.-P. Zhang, "On the shift operator, graph frequency, and optimal filtering in graph signal processing," *IEEE Trans. Sign. Proc.*, vol. 65, no. 23, pp. 6303 – 6318, 2017.
- [42] B. Seifert, C. Wendler, and M. Püschel, "Wiener Filter on Meet/Join Lattices," 2021, submitted for publication.